paper:541

Analysis of non-stationary signals in power systems

Zbigniew Leonowicz
ABSP Lab., BSI, Riken (Japan)
on leave from the Wroclaw University of Technology (Poland)

Received the M.Sc. and PhD degrees in electrical engineering from the Wroclaw University of Technology, Poland in 1997 and 2001 respectively. The NATO Organisation awarded Dr. Leonowicz an Advanced Fellowship in 2001 and he spent this fellowship at the Technical University of Dresden (Germany). He has been with the Department of Electrical Engineering at the Wroclaw University of Technology (Poland), since 1997 and with the Advanced Brain Signal Processing Laboratory, Brain Science Institute, Riken, Wako-shi (Japan), since 2003. His current research interests include modern digital signal processing methods.

Abstract:
Classical techniques to estimate the spectrum of the multi-component signal are based on Fourier-based transformations. The frequency estimates obtained from their spectral peaks are affected by the window length and phase of signal component, thus presenting a large variance even in the absence of noise.
We estimate the spectrum of the signals with the help of the Wigner-Ville distribution (WVD) and we obtain its time-frequency representation. For the same purpose, the min-norm method (subspace method) is used.
The accuracy and phase dependence of the tested methods were investigated and compared with the parameters of the frequency estimation via FFT. The proposed methods were also tested with nonstationary multiple-component signals occurring during the fault operation of inverter-fed drives and transmission lines.

Keywords: spectral analysis, Wigner-Ville distribution, min-norm, fault detection, power converter, transmission lines.

Word count: 1793

Introduction

Spectrum estimation of discretely sampled processes is usually based on procedures employing the FFT. This approach is computationally efficient and generally produces useful results for a large class of signal processes.
However, there are several performance limitations of the FFT: low frequency resolution, i.e. the ability to distinguish the spectral responses of two or more signals and limitations due to windowing of the data.
Windowing manifests as leakage in the spectral domain: energy of the main lobe of a spectral response "leaks" into the sidelobes obscuring and distorting other spectral components.
These limitations are especially troublesome when analysing short data records, which occur in practice or because processes have slowly time-varying spectra, that may be considered constant only for short record lengths.
The time-varying spectra of a nonstationary time series commonly used are the spectrogram obtained from the short-time Fourier transform (STFT) and the scalogram obtained from the wavelet transform.
Another type of time-frequency distribution is the Wigner-Ville (WV) distribution, which appears to show better frequency concentration and less phase dependence than Fourier spectra.
However, the computational requirements of that method are often significantly higher than FFT processing.
A recent method of spectrum estimation is based on the linear algebraic concepts of subspaces and so has been called "subspace method". One of the most important technique, which is based on the Pisarenko approach of separating the data into signal and noise subspaces, is the min-norm method.
The Wigner-Ville distribution is another approach that is especially appropriate for analysis of transient signals, due to its better temporal resolution than alternative spectral estimation approaches (FFT, STFT).

Subspace Methods - Min-Norm

The Min-Norm method (Therrien, 1992) involves calculation of the correlation matrix

$$\mathbf{R}_{\mathbf{x}} = \sum_{i=1}^{M} E\left\{A_i A_i^*\right\} s_i s_i^T + \sigma_0^2 \mathbf{I} \tag{1}$$

of the observed data **x** under assumption that it consists of *M* complex sinusoids in white Gaussian noise.

$$\mathbf{x} = \sum_{i=1}^{M} A_i s_i + \eta$$

where $A_i = \left|A_i\right| e^{j\phi_i}; s_i = e^{j\omega_i}$

Smallest eigenvalues of the matrix correspond to the noise subspace and the largest (all greater than the noise variance σ_0^2) correspond to the signal subspace.
The matrix of eigenvectors is defined by:

$$\mathbf{E}_{noise} = \begin{bmatrix} \mathbf{e}_{M+1} & \mathbf{e}_{M+2} & \cdots & \mathbf{e}_N \end{bmatrix} \tag{2}$$

Min-Norm method uses one vector **d** for frequency estimation. This vector, belonging to the noise subspace, has minimum Euclidean norm and its first element is equal to one. We can present $\mathbf{E}_{noise}$ in the form

$$\mathbf{E}_{noise} = \begin{bmatrix} \mathbf{c}^{*T} \\ \mathbf{E}'_{noise} \end{bmatrix} \tag{3}$$

where $\mathbf{c}^{*T}$ is the upper row of the matrix. Hence $\mathbf{c} = \mathbf{E}_{noise}^{*T} \ell$, where $\mathbf{d}^{*T} \ell = 1$. These conditions are expressed by the following equation (Therrien, 1992)

$$\mathbf{d} = \frac{1}{\mathbf{c}^{*T}\mathbf{c}} \mathbf{E}_{noise}\mathbf{c} = \begin{bmatrix} 1 \\ \left(\mathbf{E}'_{noise}\mathbf{c}\right) / \left(\mathbf{c}^{*T}\mathbf{c}\right) \end{bmatrix} \tag{4}$$

A pseudospectrum is defined with the help of **d** as:

$$\hat{P}\left(e^{j\omega}\right) = \frac{1}{\left|\mathbf{w}^{*T}\mathbf{d}\right|^2} = \frac{1}{\mathbf{w}^{*T}\mathbf{d}\mathbf{d}^{*T}\mathbf{w}} \tag{5}$$

where **w** is defined as: $\mathbf{w} \triangleq \begin{bmatrix} 1 & e^{j\omega_i} & \cdots & e^{j(N-1)\omega_i} \end{bmatrix}^T$

Since each of the elements of the signal vector is orthogonal to the noise subspace, the quantity (5) exhibits sharp peaks at the signal component frequencies.

In order to adapt this method for the analysis of non-stationary signals, a similar approach is used now as in the short-time Fourier transform (STFT). A time varying signal is first broken up into segments (with the help of the temporal window function) and each segment is then analysed. Next, the denominator of (5) is estimated for the each time instant, which enables estimates of the instantaneous frequency of the signal (Shan, 1998).

Wigner-Ville Representation

The Wigner-Ville distribution (WVD) (Qian and Chen, 1996) is the time-frequency representation given by:

$$W_x(t,\omega) = \int_{-\infty}^{\infty} x\left(t+\tfrac{\tau}{2}\right) x^*\left(t-\tfrac{\tau}{2}\right) e^{(-j\omega\tau)} \mathrm{d}\tau \tag{6}$$

where t is a time variable, ω is a frequency variable and * denotes complex conjugate.

The Wigner distribution is a two-dimensional function describing the frequency content of a signal as a function of time (Boashash, 1988) and possesses many advantageous properties, among them:

1. Instantaneous frequency property which says that, at the time instant t, the mean instantaneous frequency of the $W_x(t,\omega)$ is equal to the mean instantaneous frequency of the signal (Boashash, 1988).
2. Because the Wigner-Ville distribution satisfies both time and frequency marginal conditions, it can be shown (Boashash, 1988), that the energy content of the $W_x(t,\omega)$ is equal to that of the original signal.

Evaluation of a Wigner-Ville distribution is a non-linear operation (quadratic operation applied to the signal) followed by a linear Fourier transform. The essential difference between a Wigner-Ville distribution and a spectrogram is thus the reversed order of non-linear operation and Fourier transform. In fact, a spectrogram originates from a short-time Fourier transform with an external window function, but the Wigner-Ville distribution can be regarded as a similar analysis but with the window matched to the signal and this window is the mirror of the signal itself. Moreover, the Wigner-Ville distribution (in its original form) does not require the introduction of a window function, which remains external to the signal.

For a discrete-time signal $x(n)$ the discrete pseudo-Wigner-Ville distribution (PWD) is evaluated using a sliding symmetrical finite-length analysis window $h(\tau)$ (Qian and Chen, 1996).

$$W_{xh}(n,k) = 2\sum_{\tau=-L}^{L} x(n+\tau)x^*(n-\tau)\times h(\tau)h^*(-\tau)e^{-j4\pi k\tau/N} \tag{7}$$

where $h(\tau)$ is a windowing function that satisfies the condition: $h(\tau)=0;\ |\tau|>L$ and n and k correspond to the discrete time and frequency variables respectively.

The short-time Fourier transform (STFT) was the first tool for analysing a signal in the joint time-frequency domain. The crucial drawback inherent to the STFT is the trade-off between time and frequency resolution. WVD does not suffer from interaction between time and frequency resolutions, but presents some other undesired properties (e.g. cross-term interference). Because a WVD is a linear combination of auto- and cross correlation terms, each pair of the signal components creates one additional cross-term in the spectrum, thus confusing the desired time-frequency representation.
One way of lowering cross-term interference is to apply a low-pass filter to the WVD, but such smoothing reduces its frequency resolution (Qian and Chen, 1996).

Another way of lowering cross-term interference is to use the WVD of analytical signal[1], which avoids all cross-terms associated with negative frequency components. The analytical function, however, differs from the original signal in different ways; e.g. its instantaneous properties may substantially differ from that of the original signal (Martin and Flandrin, 1985).

[1] An analytical signal $z(t)$ can be generated from a real signal $x(t)$ as: $z(t)=x(t) + j\ \mathrm{H}[x(t)]$; where H[*] is the Hilbert transform operator, and $j^2 = -1$

Investigations

Fault operation of the converter drive

In the recent years, simulation programs for complex electrical circuits and control systems have been markedly improved. An accurate simulation of their characteristic transient phenomena is now feasible without hardware. For example, the EMTP-ATP (EMTP, 1992) (Electromagnetic Transients Program) is a FORTRAN based simulation that serves for modelling complex 1- or 3- phase networks occurring in drive, control and energy systems.

This paper shows simulation results for a 3 kVA PWM-converter with a modulation frequency of 1 kHz supplying a 2-pole, 1 kW asynchronous motor (Fig. 1)

Figure 1.

The complex space-phasor $\underline{f_p} = f_\alpha + j \cdot f_\beta$ of a three-phase system f_R, f_S, f_T is given by (Serrano, 1975)

$$\begin{bmatrix} f_\alpha \\ f_\beta \end{bmatrix} = \sqrt{\frac{2}{3}} \begin{bmatrix} 1 & -\frac{1}{2} & -\frac{1}{2} \\ 0 & \sqrt{\frac{3}{2}} & -\sqrt{\frac{3}{2}} \end{bmatrix} \begin{bmatrix} f_R \\ f_S \\ f_T \end{bmatrix} \tag{8}$$

It describes, in addition to the positive-sequence component, an existing negative-sequence component, harmonic as well as non-harmonic frequency components of the signal. The complex space-phasor of the converter output 3-phase currents is investigated using the previously cited spectrum estimation methods.

The time-frequency representation of the space-phasor is considered by reference to:

1. Fault operation of the inverter drive - Increase of the motor lead resistance to 100 Ω. Main frequency of the inverter 120 Hz, sampling frequency 20 kHz.

Figure 2

2. Fault operation of the inverter drive - short-circuit between motor leads. Main frequency of the inverter 60 Hz, sampling frequency 20 kHz.

Figure 3

Time-frequency representation of the time varying signals (Fig. 2, 3) obtained with the help of the min-norm method and spectrogram is presented on fig. 8-16. Each line of the time-frequency representation is obtained from the time interval of 40 samples.

Results:

1. Fault operation of the inverter drive - Increase of the motor lead resistance

Figure 4
Figure 5
Figure 6

2. Fault operation of the inverter drive - Short-circuit between motor leads.

Figure 7

In Fig. 4-6 we can see a simple case of supply asymmetry at the motor. After the fault, a negative component with frequency 120 Hz is caused by asymmetric state. We can also see a positive intermodulation component with frequency 760 Hz (1000 Hz (PWM modulation frequency) - 2120 Hz = 760 Hz) and negative intermodulation component with frequency -1240 Hz (1000 Hz + 2120 Hz = 1240 Hz). In contrast, the spectrogram shows only the main frequency component (120 Hz) (Fig. 5, 6).

In the case, where a short circuit occurs between the motor leads, (Fig.7) shows additional intermodulation components.

Wigner-Ville representation of the short-circuit waveform

Investigated waveform appears during the single line to ground fault in the transmission line. At the time of fault 50 ms appears an exponentially damped component with frequency 130 Hz.

Figure 8.

Results:
The Wigner-Ville distribution of the signal in Fig. 8 is shown in Fig. 9. Analytical form of the signal is used. WVD offers the possibility to track the frequency and amplitude changes of non-stationary signals.
In figure 10 is shown the estimated instantaneous frequency of the signal in figure 8.
Figure 9.
Figure 10.
In Figure 11 is shown the estimated instantaneous amplitude (power) of the main component. Both characteristics show good correlation with the true changes of investigated signal.
Figure 11.

Conclusions

Modern frequency power converters generate a wide spectrum of harmonic components. Large converter systems can also generate non-characteristic harmonics and interharmonics. These are not revealed by standard tools of harmonic analysis based on the Fourier transform whose harmonics have periodicity intervals of 20 ms (50 Hz) and submultiples. On the other hand, the periodicities of the interharmonics (when they exist) can be variable and much longer.
Visualisation of frequency converter supplied drives by means of a static space-phasor is a very useful, compact observation and diagnostic method. The spectrum of the space-phasor and of the real-valued signal has been investigated under different operation conditions using the min-norm method and Wigner-Ville distribution. Superiority of the proposed approaches over the conventional FFT-based tool has been shown. In addition, the detection of irregular frequencies may be useful for the diagnosis of some drive faults. The WVD either allows the possibility to track the frequency and amplitude changes of non-stationary signals.

Acknowledgment

This work was partly supported by the North Atlantic Treaty Organization (Advanced Science Fellowship for Dr Zbigniew Leonowicz).

References

Boashash B.(1988) „Note on the use of the Wigner distribution for time-frequency signal analysis" , IEEE Trans. Acoustics, Speech, Signal Processing, Vol. 36, No 9, pp. 1518-1521

Cohen L. (1995), Time-Frequency Analysis, Prentice-Hall, Englewood Cliffs.

EMTP-ATP Rule Book(1992) , Canadian-American User Group, 1987-1992.

Lobos T., Kozina T., Koglin H.-J. (2001): "Power System Harmonics Estimation Using Linear Least Squares Method and SVD", IEE Proc.-Gener. Transm. Distrib., vol. 148, No. 6, pp. 567- 572.

Martin W.(1985), Flandrin P., „Wigner-Ville Spectral Analysis of Nonstationary Processes", IEEE Trans. on Acoustics, Speech and Signal Processing, Vol. Assp. 33, No. 4, pp. 1461-1470.

Quian S., Chen D.(1996), Joint Time-Frequency Analysis, Upper Saddle River, Prentice Hall PTR, pp 45-75 & 101-131.

Serrano-Iribarnegaray L.(1975): „The modern space-phasor theory, Part I,1st coherent formulation and its advantages for transient analysis of converter-fed AC machines", ETEP, vol. 3, No. 3, pp. 171-180.

Shan P., Beex A. A.(1998): „High-resolution instantaneous frequency estimation based on time-varying AR modelling", Proceedings of the IEEE-SP Int. Symposium on Time-Frequency and Time-Scale Analysis, Pittsburgh, pp.109-112.

Therrien C.W. (1992), Discrete Random Signals and Statistical Signal Processing. Prentice Hall, Englewood Cliffs, New Jersey, 1992.

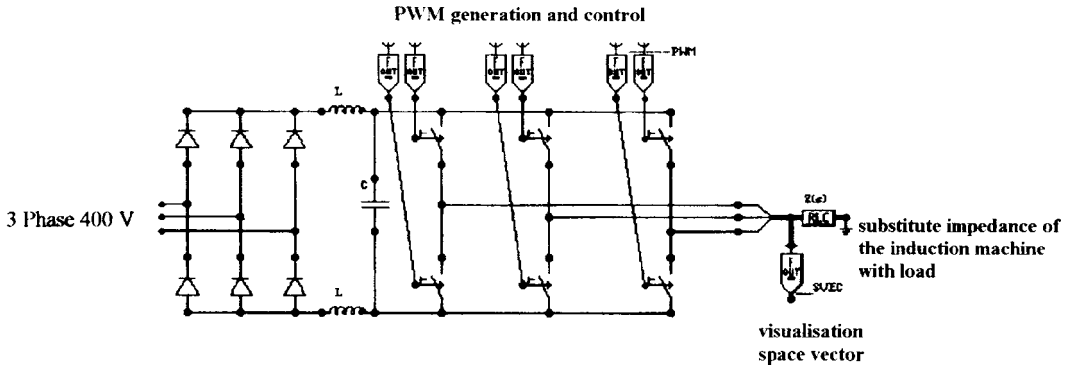

Fig. 1. Simulated PWM converter.

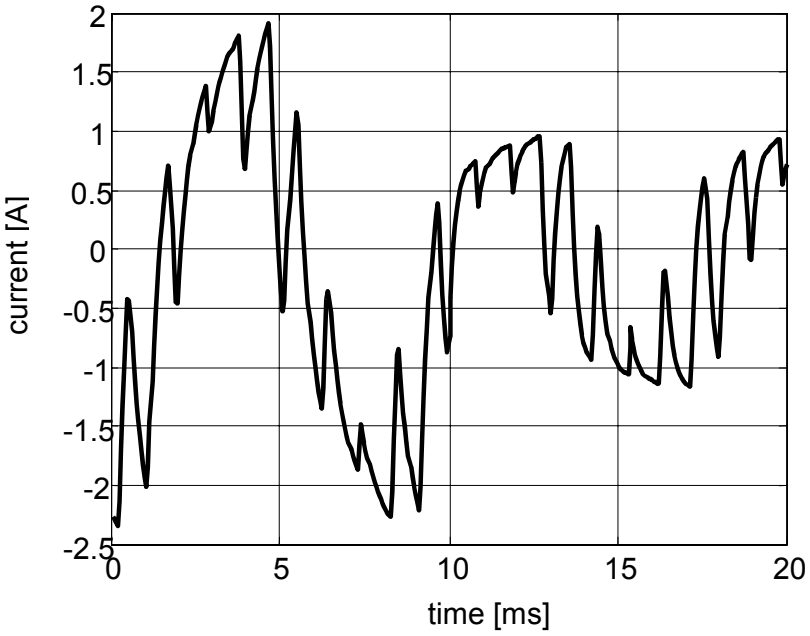

Fig. 2. Fault operation 1 of the inverter drive (phase R). Fault occurs at time 10 ms.

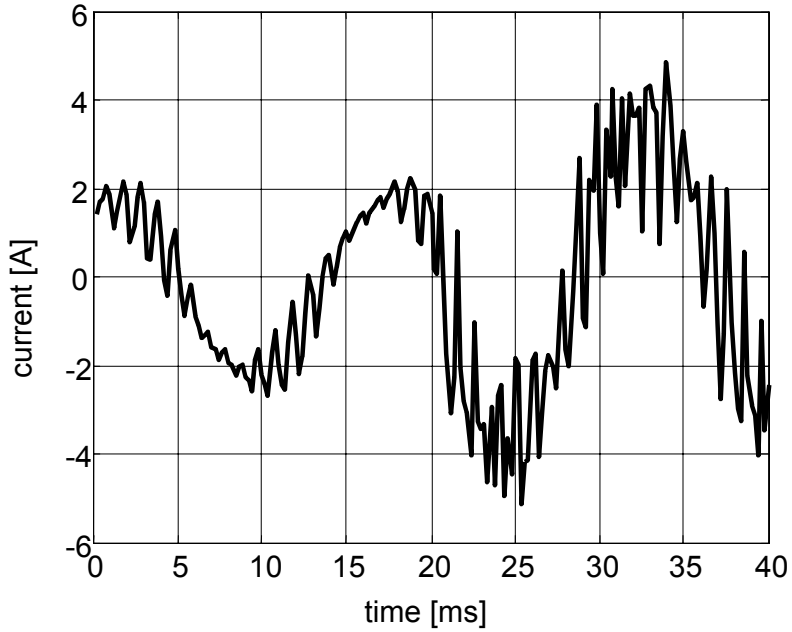

Fig. 3. Fault operation 2 of the inverter drive (phase R). fault occurs at time 20 ms.

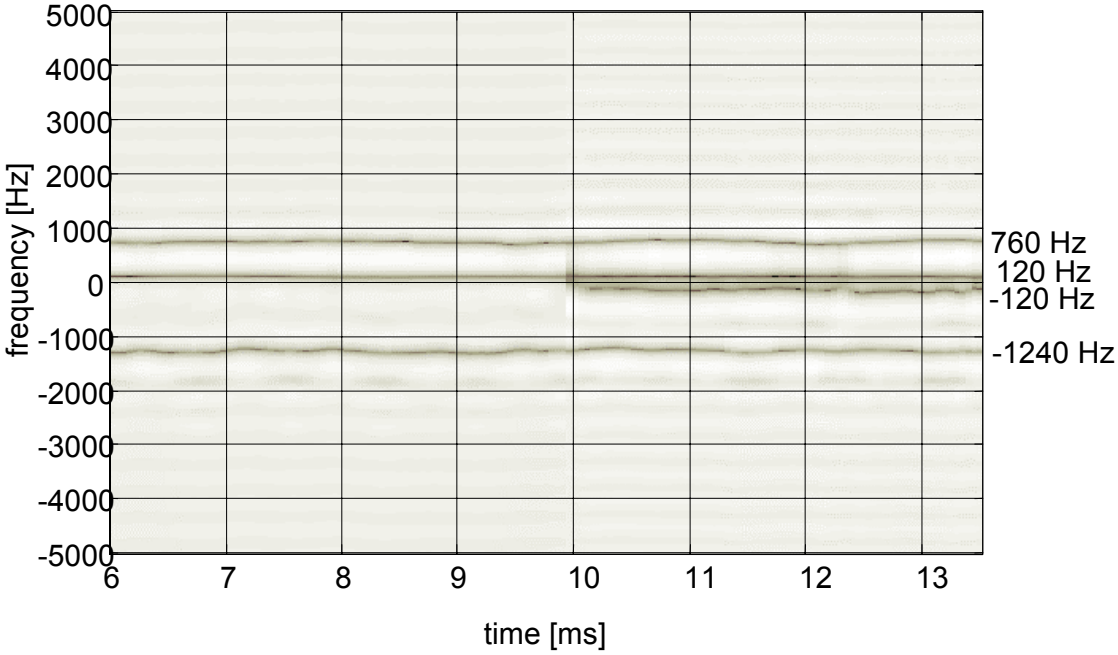

Fig. 4. Min-Norm representation of the signal from Fig. 2.

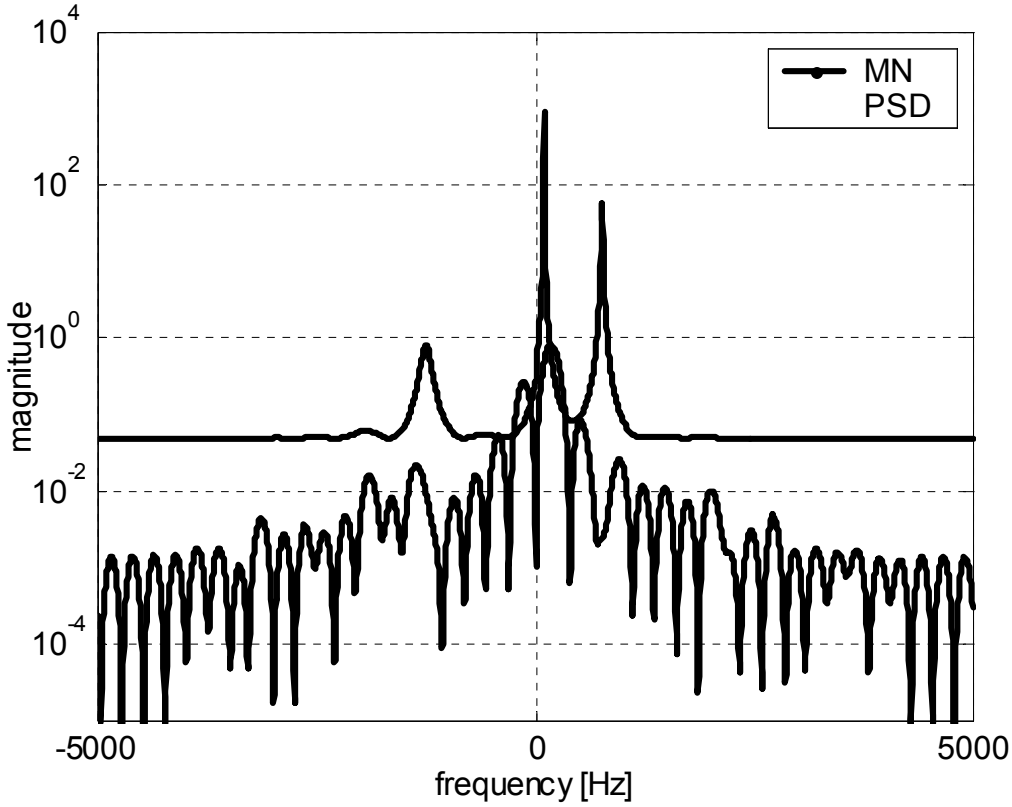

Fig. 5. Slice of the MN and PSD representations of the signal from Fig. 2 for time=8 ms.

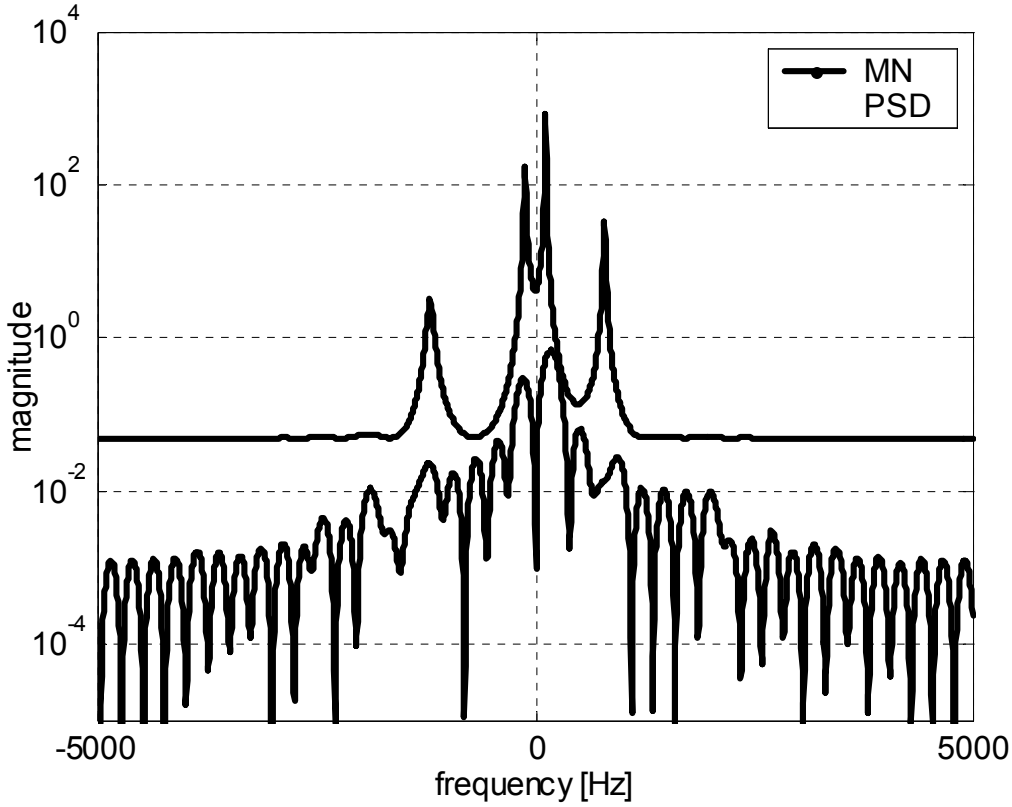

Fig. 6. Slice of the MN and PSD representations of the signal from Fig. 2 for time=12 ms.

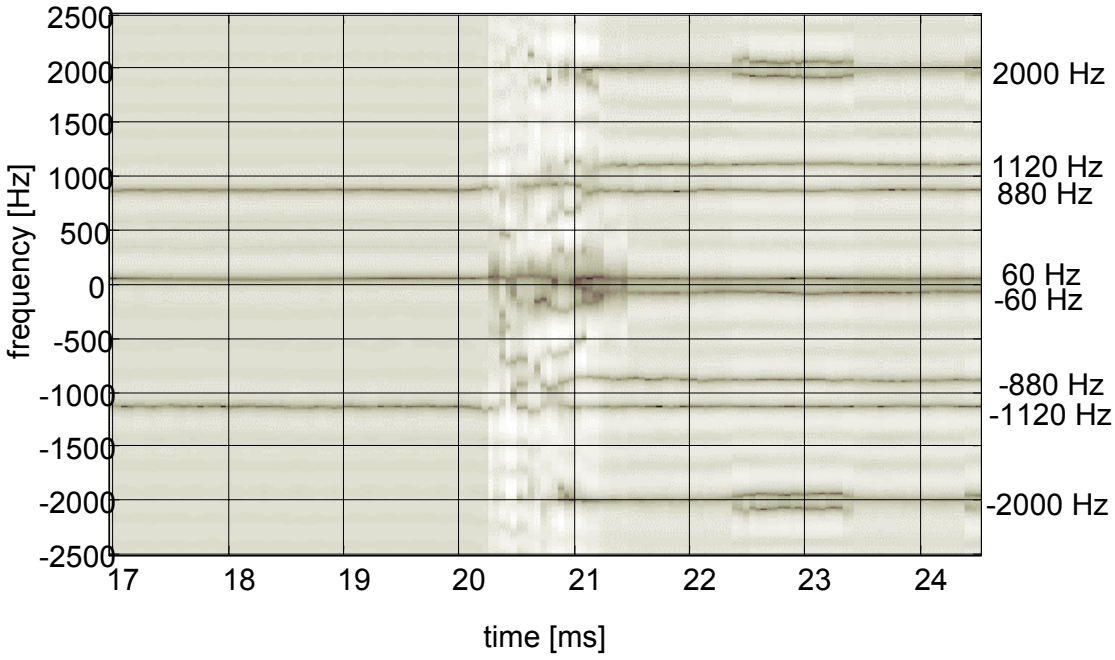

Fig. 7. Min-Norm representation of the signal from Fig. 3.

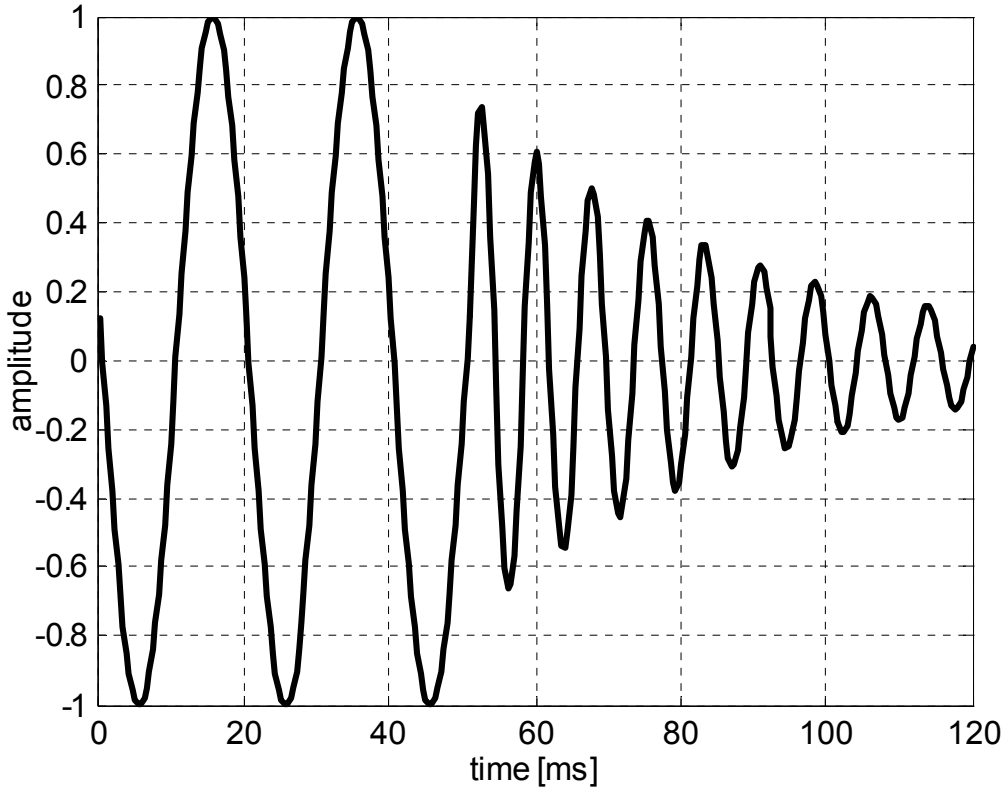

Fig. 8. Short-circuit waveform.

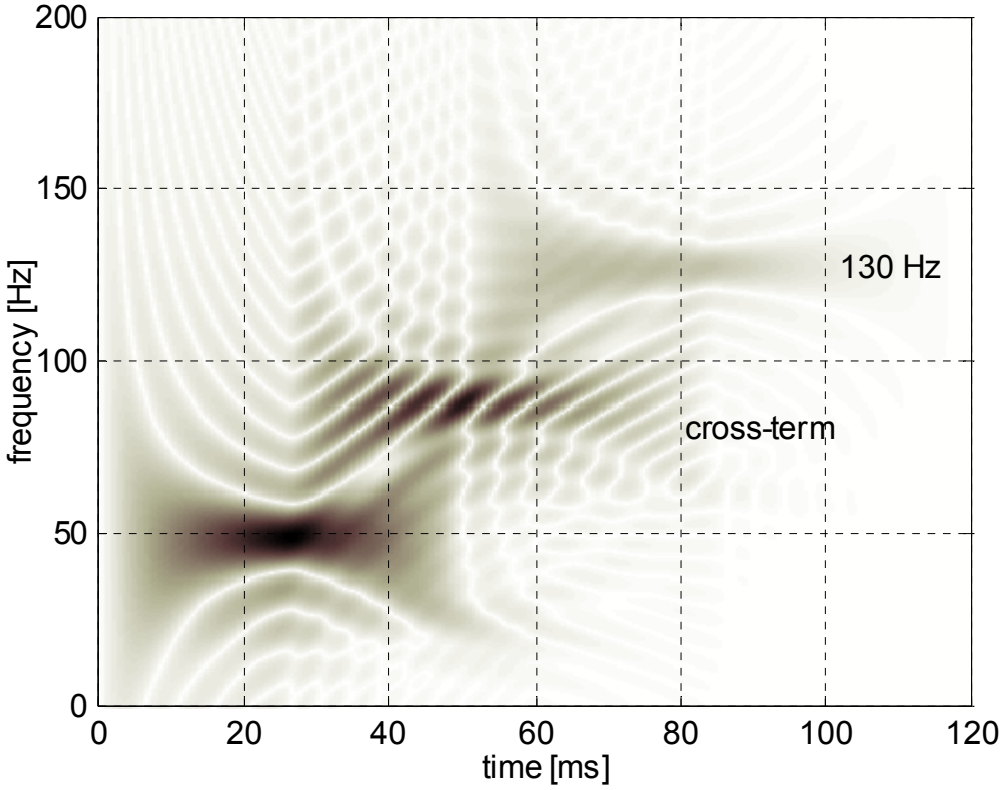

Fig. 9. The Wigner-Ville distribution of the signal in Fig. 8.

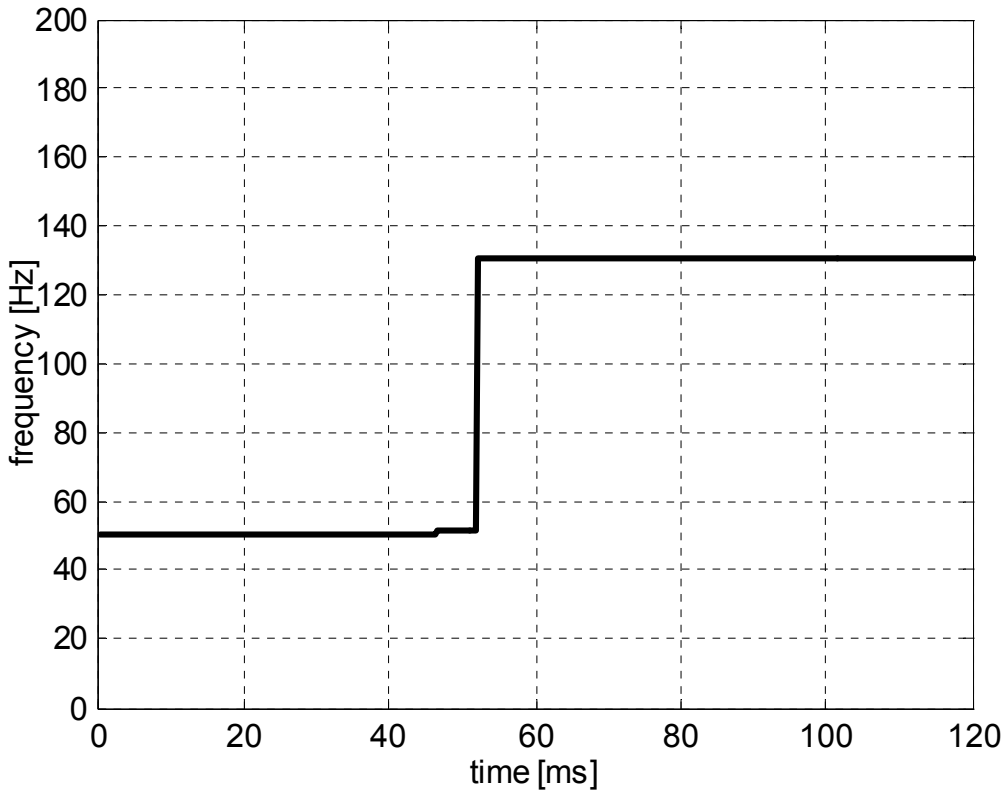

Fig. 10. Estimated instantaneous frequency of the signal in figure 8.

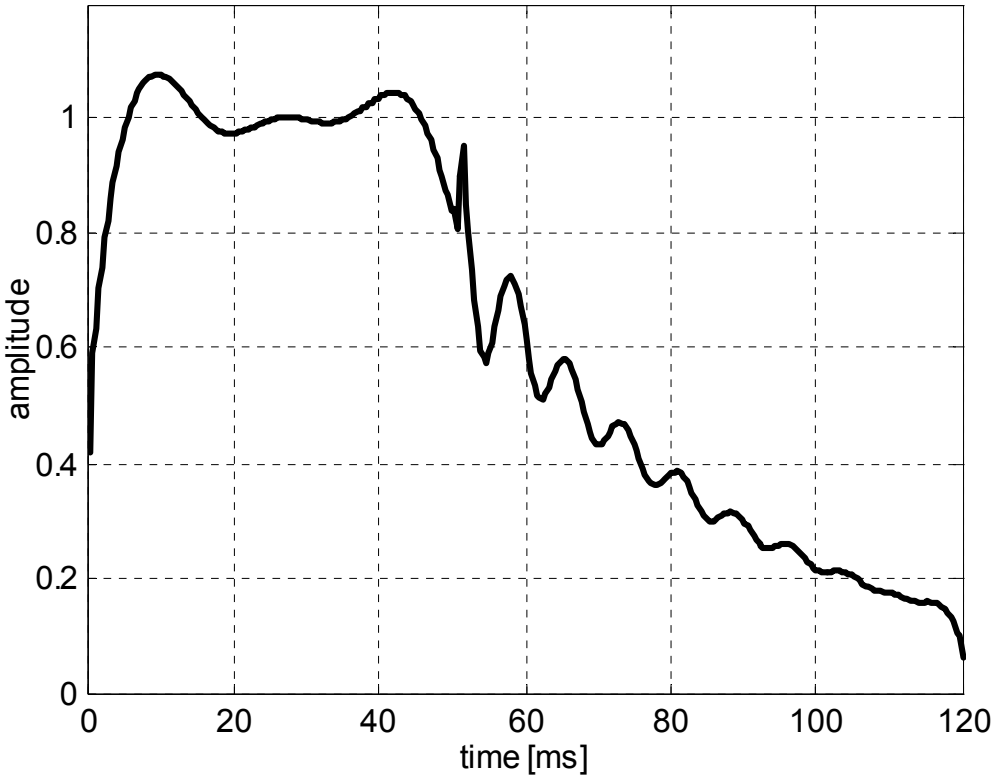

Fig. 11. Estimated instantaneous amplitude of the signal in figure 8.